axioms

MDPI

Article

A Weighted Cosine-G Family of Distributions: Properties and Illustration Using Time-to-Event Data

Omalsad Hamood Odhah [1], Huda M. Alshanbari [1], Zubair Ahmad [2,*] and Gadde Srinivasa Rao [3]

[1] Department of Mathematical Sciences, College of Science, Princess Nourah bint Abdulrahman University, P.O. Box 84428, Riyadh 11671, Saudi Arabia; ohodhah@pnu.edu.sa (O.H.O.); hmalshanbari@pnu.edu.sa (H.M.A.)
[2] Department of Statistics, Quaid-i-Azam University, Islamabad 44000, Pakistan
[3] Department of Mathematics and Statistics, University of Dodoma, Dodoma P.O. Box 259, Tanzania; gaddesrao@gmail.com
* Correspondence: z.ferry21@gmail.com; Tel.: +92-345-9375162

Abstract: Modeling and predicting time-to-event phenomena in engineering, sports, and medical sectors are very crucial. Numerous models have been proposed for modeling such types of data sets. These models are introduced by adding one or more parameters to the traditional distributions. The addition of new parameters to the traditional distributions leads to serious issues, such as estimation consequences and re-parametrization problems. To avoid such problems, this paper introduces a new method for generating new probability distributions without any additional parameters. The proposed method may be called a weighted cosine-*G* family of distributions. Different distributional properties of the weighted cosine-*G* family, along with the maximum likelihood estimators, are obtained. A special model of the weighted cosine-*G* family, by utilizing the Weibull model, is considered. The special model of the weighted cosine-*G* family may be called a weighted cosine-Weibull distribution. A simulation study of the weighted cosine-Weibull model is conducted to evaluate the performances of its estimators. Finally, the applications of the weighted cosine-Weibull distribution are shown by considering three data sets related to the time-to-event phenomena.

Keywords: cosine function; trigonometric function; Weibull distribution; distributional properties; simulation; time-to-event data; statistical modeling

MSC: 62N01, 62N02

Citation: Odhah, O.H.; Alshanbari, H.M.; Ahmad, Z.; Rao, G.S. A Weighted Cosine-G Family of Distributions: Properties and Illustration Using Time-to-Event Data. *Axioms* **2023**, *12*, 849. https://doi.org/10.3390/axioms12090849

Academic Editor: Angel Ricardo Plastino

Received: 15 June 2023
Revised: 3 August 2023
Accepted: 13 August 2023
Published: 30 August 2023

1. Introduction

The literature on distribution theory contains a series of probability distributions for analyzing and predicting real phenomena in various applied areas, such as the healthcare and biomedical sectors, engineering sector, actuarial and management sciences, education, and hydrology [1–8]. However, no particular probability model is appropriate for analyzing and predicting every phenomenon. Therefore, every year, the impetus to develop new probability models with higher distributional flexibility is growing [9].

The increased interest of researchers in data analysis and modeling motivates researchers to look for new approaches (new family of distributions). Therefore, researchers have been trying to look for new methods to obtain updated versions of the existing models with greater distributional flexibility. Most of the new methods developed for the derivation of new probability distributions contain additional parameters, ranging from one to seven or more [10]. As the number of the parameters increases, the new resultant probability model faces two major problems: (i) the fact that estimation consequences arise, and (ii) re-parametrization.

There are only a few methods that are developed without any additional parameters. In this regard, Kumar et al. [11] introduced a new class of distribution by combining a baseline cumulative distribution function (CDF) with a sine function, named the SS transformation. For any baseline CDF $G(t;\boldsymbol{\eta})$, this is defined as $F(t;\boldsymbol{\eta}) = \sin\left[\frac{\pi}{2}G(t;\boldsymbol{\eta})\right]$, where $\boldsymbol{\eta}$ is a parameter vector. Mahmood et al. [12] proposed another family of distributions using a trigonometric function, called a new sine-G family. For any baseline $G(t;\boldsymbol{\eta})$, a new sine-G family is defined as $F(t;\boldsymbol{\eta}) = \sin\left[\frac{\pi}{4}G(t;\boldsymbol{\eta})(1+G(t;\boldsymbol{\eta}))\right]$. Another contribution to such families of distributions was introduced by Ampadu [13], by means of developing the hyperbolic Tan-X family. For any baseline $G(t;\boldsymbol{\eta})$, the hyperbolic Tan-X family is defined as $F(t;\boldsymbol{\eta}) = Tanh[3\pi G(t;\boldsymbol{\eta})]$. For more studies on the development of probabilistic models based on trigonometric functions, please refer to [14–18].

Taking motivation from the above discussion, we also propose a new method for obtaining new probability models without adding additional parameters. The proposed method may be called weighted cosine-G (WC-G) distributions. The WC-G method significantly improves the fitting power of the existing models, as is shown in Section 5.

Definition 1. *Let $S(t;\boldsymbol{\eta})$ be the survival function (SF) of a continuous baseline probability model having CDF $G(t;\boldsymbol{\eta})$ and probability density function (PDF) $g(t;\boldsymbol{\eta})$; that is $S(t;\boldsymbol{\eta}) = 1 - G(t;\boldsymbol{\eta})$. Then, the CDF $F(t;\boldsymbol{\eta})$ of the WC-G family is given by*

$$F(t;\boldsymbol{\eta}) = \frac{e^{\left(1-\cos\left[\frac{\pi G(t;\boldsymbol{\eta})}{1+G(t;\boldsymbol{\eta})}\right]\right)} - 1}{e-1}, \qquad t \in \mathbb{R}, \tag{1}$$

with PDF $f(t;\boldsymbol{\eta})$ is

$$f(t;\boldsymbol{\eta}) = \frac{\pi g(t;\boldsymbol{\eta}) \sin\left[\frac{\pi G(t;\boldsymbol{\eta})}{1+G(t;\boldsymbol{\eta})}\right]}{(e-1)[1+G(t;\boldsymbol{\eta})]^2} e^{\left(1-\cos\left[\frac{\pi G(t;\boldsymbol{\eta})}{1+G(t;\boldsymbol{\eta})}\right]\right)}, \qquad t \in \mathbb{R}, \tag{2}$$

where $g(t;\boldsymbol{\eta}) = \frac{d}{dt}G(t;\boldsymbol{\eta})$.

Furthermore, the survival function (SF) $S(t;\boldsymbol{\eta})$, hazard function (HF) $h(t;\boldsymbol{\eta})$, and cumulative HF $H(t;\boldsymbol{\eta})$ of the WC-G distributions are given by

$$S(t;\boldsymbol{\eta}) = \frac{e - e^{\left(1-\cos\left[\frac{\pi G(t;\boldsymbol{\eta})}{1+G(t;\boldsymbol{\eta})}\right]\right)}}{e-1}, \qquad t \in \mathbb{R},$$

$$h(t;\boldsymbol{\eta}) = \frac{\pi g(t;\boldsymbol{\eta}) \sin\left[\frac{\pi G(t;\boldsymbol{\eta})}{1+G(t;\boldsymbol{\eta})}\right]}{[1+G(t;\boldsymbol{\eta})]^2\left(e - e^{\left(1-\cos\left[\frac{\pi G(t;\boldsymbol{\eta})}{1+G(t;\boldsymbol{\eta})}\right]\right)}\right)} e^{\left(1-\cos\left[\frac{\pi G(t;\boldsymbol{\eta})}{1+G(t;\boldsymbol{\eta})}\right]\right)}, \qquad t \in \mathbb{R},$$

and

$$H(t;\boldsymbol{\eta}) = -\log\left(\frac{e - e^{\left(1-\cos\left[\frac{\pi G(t;\boldsymbol{\eta})}{1+G(t;\boldsymbol{\eta})}\right]\right)}}{e-1}\right), \qquad t \in \mathbb{R},$$

respectively.

The next section introduces a special member of the WC-G family, called the weighted cosine-Weibull (WC-Weibull) distribution. The WC-Weibull distribution is obtained by taking the Weibull model as a baseline model of the WC-G family. Some basic functions of the WC-Weibull distribution are provided in Section 2. Furthermore, visual illustrations (including the plots of PDF and HF) of the WC-Weibull distribution are also provided. Different distributional properties of the WC-Weibull distribution are derived. A simulation study of the WC-Weibull distribution is conducted for three different sets of parameters to evaluate the performances of the estimators. The evaluation of the estimators of the WC-Weibull distribution is conducted by adopting two criteria, called the mean square error and average bias. Then, we show the applicability of the WC-Weibull distribution by considering two data sets from the medical sector.

2. The WC-Weibull Distribution

Here, we provide a complete description of the WC-Weibull distribution with support $(0,\infty)$ using $G(t;\boldsymbol{\eta})$ as a CDF of the Weibull model given by

$$G(t;\boldsymbol{\eta}) = 1 - e^{-\gamma t^{\theta}}, \qquad t \geq 0, \theta, \gamma > 0, \tag{3}$$

with PDF

$$g(t;\boldsymbol{\eta}) = \theta\gamma t^{\theta-1} e^{-\gamma t^{\theta}}, \qquad t > 0,$$

where $\boldsymbol{\eta} = (\theta, \gamma)$.

Thus, our goal is to construct an updated form of Equation (3) with greater distributional flexibility. Using Equation (3) in Equation (1), we obtain the CDF $F(t;\boldsymbol{\eta})$ of the WC-Weibull distribution, given by

$$F(t;\boldsymbol{\eta}) = \frac{e^{\left(1-\cos\left[\frac{\pi\left(1-e^{-\gamma t^{\theta}}\right)}{2-e^{-\gamma t^{\theta}}}\right]\right)} - 1}{e-1}, \qquad t \geq 0, \tag{4}$$

and PDF $f(t;\boldsymbol{\eta})$

$$f(t;\boldsymbol{\eta}) = \frac{\pi\theta\gamma t^{\theta-1} e^{-\gamma t^{\theta}} \sin\left[\frac{\pi\left(1-e^{-\gamma t^{\theta}}\right)}{2-e^{-\gamma t^{\theta}}}\right]}{(e-1)\left[2-e^{-\gamma t^{\theta}}\right]^2} e^{\left(1-\cos\left[\frac{\pi\left(1-e^{-\gamma t^{\theta}}\right)}{2-e^{-\gamma t^{\theta}}}\right]\right)}, \qquad t > 0. \tag{5}$$

Furthermore, the SF and HF of the WC-Weibull distribution are, respectively, expressed by

$$S(t;\boldsymbol{\eta}) = \frac{e - e^{\left(1-\cos\left[\frac{\pi\left(1-e^{-\gamma t^{\theta}}\right)}{2-e^{-\gamma t^{\theta}}}\right]\right)}}{e-1}, \qquad t > 0,$$

and

$$h(t;\boldsymbol{\eta}) = \frac{\pi\theta\gamma t^{\theta-1} e^{-\gamma t^{\theta}} \sin\left[\frac{\pi\left(1-e^{-\gamma t^{\theta}}\right)}{2-e^{-\gamma t^{\theta}}}\right]}{\left(e - e^{\left(1-\cos\left[\frac{\pi\left(1-e^{-\gamma t^{\theta}}\right)}{2-e^{-\gamma t^{\theta}}}\right]\right)}\right)\left[2-e^{-\gamma t^{\theta}}\right]^2} e^{\left(1-\cos\left[\frac{\pi\left(1-e^{-\gamma t^{\theta}}\right)}{2-e^{-\gamma t^{\theta}}}\right]\right)}, \qquad t > 0.$$

To show the distributional flexibility of the WC-Weibull distribution, we provide some graphs of the PDF $f(t;\boldsymbol{\eta})$ of the WC-Weibull distribution in Figure 1. The plots of $f(t;\boldsymbol{\eta})$ of the WC-Weibull distribution are obtained for (i) $\theta = 2.9$, and $\gamma = 0.3$ (red curve), (ii) $\theta = 2.5$, and $\gamma = 2.8$ (blue curve), (iii) $\theta = 0.5$, and $\gamma = 2.9$ (black curve), and (iv) $\theta = 7.2$, and $\gamma = 0.005$ (green curve). From the plots of $f(t;\boldsymbol{\eta})$ of the WC-Weibull distribution, it is obvious that the WC-Weibull distribution is very flexible, as it captures the following four different patterns of $f(t;\boldsymbol{\eta})$: (i) symmetrical pattern (red curve), (ii) right-skewed pattern (blue curve), (iii) decreasing pattern (black curve), and (iv) left-skewed pattern (green curve).

Furthermore, the plots of $h(t;\boldsymbol{\eta})$ of the WC-Weibull distribution are also presented in Figure 1. The plots of $h(t;\boldsymbol{\eta})$ of the WC-Weibull distribution are obtained for (i) $\theta = 0.4$, and $\gamma = 1.2$ (red curve), (ii) $\theta = 1.1$, and $\gamma = 1.3$ (gold curve), (iii) $\theta = 0.5$, and $\gamma = 2.9$ (black curve), (iv) $\theta = 1.01$, and $\gamma = 0.8$ (green curve), and (v) $\theta = 1.01$, and $\gamma = 0.6$ (blue curve). From the plots of $h(t;\boldsymbol{\eta})$ of the WC-Weibull distribution, it is obvious that the WC-Weibull distribution captures the following different patterns of $h(t;\boldsymbol{\eta})$: (i) increasing patterns (green and gold curves), (ii) decreasing patterns (black and red curves), and (iii) unimodal pattern (blue curve).

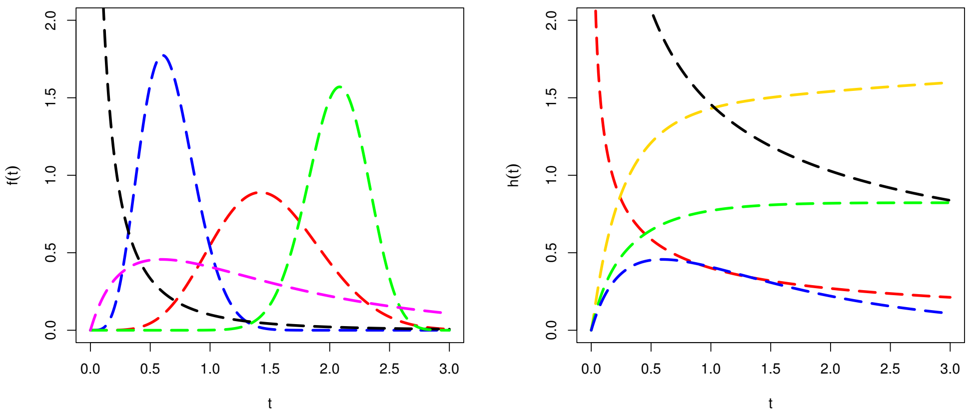

Figure 1. The plots of $f(t;\boldsymbol{\eta})$ and $h(t;\boldsymbol{\eta})$ of the WC-Weibull model for different values of θ and γ.

3. Distributional Properties

In this section, we derive some distributional properties of the WC-G family of distributions. These properties include the quantile function, quartiles, skewness, kurtosis, and the r^{th} moment. The motivation for deriving the quantiles, moments and other properties of the distribution is to study the characteristics and nature of the distribution. These are useful to obtain skewness and kurtosis of the distribution. Based on the measure of skewness, one can study the nature of the distribution, such as the symmetric or asymmetric curve of the distribution. Similarly, the peakedness of the distribution can be studied based on the measure of kurtosis, namely mesokurtic, platykurtic, or leptokurtic.

3.1. The Quantile Function

The quantile function (QF) of the WC-G family of distributions, say $Q(u)$, is given by

$$Q(u) = G^{-1}\left(\frac{\cos^{-1}(1-\log[u(e-1)+1])}{\pi - \cos^{-1}(1-\log[u(e-1)+1])}\right), \tag{6}$$

where $0 < u < 1$.

The expression in Equation (6) shows that the QF of the WC-G distributions is in an explicit form, which helps to generate random numbers easily.

3.2. The Median and Quartile Measures

The median (which is also known as the second quartile) of the WC-G distributions is obtained by replacing $u = \frac{1}{2}$ in Equation (6), as given by

$$Q\left(\frac{1}{2}\right) = G^{-1}\left(\frac{\cos^{-1}\left(1-\log\left[\frac{1}{2}(e-1)+1\right]\right)}{\pi - \cos^{-1}\left(1-\log\left[\frac{1}{2}(e-1)+1\right]\right)}\right).$$

Furthermore, the 1st quartile and 3rd quartile of the WC-G distributions are obtained, respectively, by using $u = \frac{1}{4}$ and $u = \frac{3}{4}$ in Equation (6). Henceforth, the 1st quartile and 3rd quartile of the WC-G distributions are given, respectively, by

$$Q\left(\frac{1}{4}\right) = G^{-1}\left(\frac{\cos^{-1}\left(1-\log\left[\frac{1}{4}(e-1)+1\right]\right)}{\pi-\cos^{-1}\left(1-\log\left[\frac{1}{4}(e-1)+1\right]\right)}\right),$$

and

$$Q\left(\frac{3}{4}\right) = G^{-1}\left(\frac{\cos^{-1}\left(1-\log\left[\frac{3}{4}(e-1)+1\right]\right)}{\pi-\cos^{-1}\left(1-\log\left[\frac{3}{4}(e-1)+1\right]\right)}\right).$$

The skewness (the Galton's skewness (GS)) of the WC-G distributions is obtained as follows:

$$GS = \frac{Q_{6/8} - 2Q_{4/8} + Q_{2/8}}{Q_{6/8} - Q_{2/8}},$$

where the quantities $Q_{6/8}, Q_{4/8}$, and $Q_{2/8}$ can be obtained by using $u = \frac{6}{8}, \frac{4}{8}$, and $u = \frac{2}{8}$ in Equation (6), respectively.

The kurtosis (the Moor's kurtosis (MK)) of the WC-G distributions is obtained as follows:

$$MK = \frac{Q_{7/8} - Q_{5/8} - Q_{1/8} + Q_{3/8}}{Q_{6/8} - Q_{2/8}},$$

where the quantities $Q_{7/8}, Q_{5/8}, Q_{1/8}$, and $Q_{3/8}$ can be obtained by using $u = \frac{7}{8}, \frac{5}{8}, \frac{1}{8}$, and $u = \frac{3}{8}$ in Equation (6), respectively.

3.3. The r^{th} Moment

The r^{th} moment of the WC-G distributed random variable T with PDF $f(t;\boldsymbol{\eta})$, say μ'_r, is derived as

$$\mu'_r = \int_{\Omega} t^r f(t;\boldsymbol{\eta}) dt. \tag{7}$$

Using Equation (2) in Equation (7), we obtain

$$\mu'_r = \int_{\Omega} t^r \frac{\pi g(t;\boldsymbol{\eta}) \sin\left[\frac{\pi G(t;\boldsymbol{\eta})}{1+G(t;\boldsymbol{\eta})}\right]}{(e-1)[1+G(t;\boldsymbol{\eta})]^2} e^{\left(1-\cos\left[\frac{\pi G(t;\boldsymbol{\eta})}{1+G(t;\boldsymbol{\eta})}\right]\right)} dt. \tag{8}$$

As we know that

$$e^x = \sum_{i=1}^{\infty} \frac{x^i}{i!}. \tag{9}$$

Using $x = \left(1-\cos\left[\frac{\pi G(t;\boldsymbol{\eta})}{1+G(t;\boldsymbol{\eta})}\right]\right)$ in Equation (9), we obtain

$$e^{\left(1-\cos\left[\frac{\pi G(t;\boldsymbol{\eta})}{1+G(t;\boldsymbol{\eta})}\right]\right)} = \sum_{i=1}^{\infty} \frac{\left(1-\cos\left[\frac{\pi G(t;\boldsymbol{\eta})}{1+G(t;\boldsymbol{\eta})}\right]\right)^i}{i!},$$

or

$$e^{\left(1-\cos\left[\frac{\pi G(t;\boldsymbol{\eta})}{1+G(t;\boldsymbol{\eta})}\right]\right)} = \sum_{i=1}^{\infty}\sum_{j=0}^{i} (-1)^j \binom{i}{j} \frac{\left(\cos\left[\frac{\pi G(t;\boldsymbol{\eta})}{1+G(t;\boldsymbol{\eta})}\right]\right)^j}{i!}. \tag{10}$$

We also know that

$$\frac{1}{(1+x)^2} = \sum_{k=1}^{\infty} (-1)^k k x^{k-1}. \tag{11}$$

Using $x = [1 + G(t;\boldsymbol{\eta})]$ in Equation (11), we derive

$$\frac{1}{[1+G(t;\boldsymbol{\eta})]^2} = \sum_{k=1}^{\infty} (-1)^k k [1+G(t;\boldsymbol{\eta})]^{k-1},$$

or

$$\frac{1}{[1+G(t;\boldsymbol{\eta})]^2} = \sum_{k=1}^{\infty} \sum_{m=0}^{k} k(-1)^k \binom{k-1}{m} [G(t;\boldsymbol{\eta})]^m. \tag{12}$$

Using Equations (10) and (12) in Equation (8), we obtain

$$\mu_r' = \pi \sum_{i=1}^{\infty} \sum_{j=0}^{i} \sum_{k=1}^{\infty} \sum_{m=0}^{k} \frac{\pi k(-1)^{j+k} \binom{i}{j} \binom{k-1}{m}}{(e-1)} \int_{\Omega} t^r g(t;\boldsymbol{\eta}) [G(t;\boldsymbol{\eta})]^m \sin\left[\frac{\pi G(t;\boldsymbol{\eta})}{1+G(t;\boldsymbol{\eta})}\right]$$
$$\times \left(\cos\left[\frac{\pi G(t;\boldsymbol{\eta})}{1+G(t;\boldsymbol{\eta})}\right]\right)^j dt,$$

$$\mu_r' = \pi \sum_{i=1}^{\infty} \sum_{j=0}^{i} \sum_{k=1}^{\infty} \sum_{m=0}^{k} \frac{\pi k(-1)^{j+k} \binom{i}{j} \binom{k-1}{m}}{(e-1)} \kappa_{r,i,j,k,m}(t;\boldsymbol{\eta}),$$

where

$$\kappa_{r,i,j,k,m}(t;\boldsymbol{\eta}) = \int_{\Omega} t^r g(t;\boldsymbol{\eta}) [G(t;\boldsymbol{\eta})]^m \sin\left[\frac{\pi G(t;\boldsymbol{\eta})}{1+G(t;\boldsymbol{\eta})}\right] \left(\cos\left[\frac{\pi G(t;\boldsymbol{\eta})}{1+G(t;\boldsymbol{\eta})}\right]\right)^j dt.$$

For different values of θ and γ, the numerical description of the moments, coefficient of variation (CV), skewness, and kurtosis of the WC-Weibull distribution are presented in Table 1.

Table 1. Numerical description of certain key measures of the WC-Weibull distribution.

Parameters		**Measures**							
γ	θ	μ_1'	μ_2'	μ_3'	μ_4'	σ^2	**CV**	**Skewness**	**Kurtosis**
0.25	0.5	39.8608	7667.83	3.66955×10^6	3.28445×10^9	6078.95	1.956	36.9047	74.8206
	1.0	4.82182	39.8608	480.029	7667.83	16.6109	0.845251	3.55452	8.51061
	2.0	2.02246	4.82182	13.123	39.8608	0.731455	0.422876	0.434448	3.44383
	3.0	1.56719	2.65779	4.82182	9.27623	0.201703	0.286572	0.0722435	2.92154
0.7	0.5	5.08429	124.75	7614.9	869357.	98.9	1.956	36.9047	74.8206
	1.0	1.72208	5.08429	21.8672	124.75	2.11874	0.845251	3.55452	8.51061
	2.0	1.20865	1.72208	2.80088	5.08429	0.261234	0.422876	0.434448	3.44383
	3.0	1.11191	1.33787	1.72208	2.3505	0.101533	0.286572	0.0722435	2.92154
2.0	0.5	0.622826	1.87203	13.9982	195.768	1.48412	1.956	36.9047	74.8206
	1.0	0.602727	0.622826	0.937557	1.87203	0.259545	0.845251	3.55452	8.51061
	2.0	0.715049	0.602727	0.579959	0.622826	0.0914319	0.422876	0.434448	3.44383
	3.0	0.783595	0.664447	0.602727	0.579765	0.0504257	0.286572	0.0722435	2.92154
3.0	0.5	0.276811	0.369784	1.22892	7.63857	0.293159	1.956	36.9047	74.8206
	1.0	0.401818	0.276811	0.277795	0.369784	0.115354	0.845251	3.55452	8.51061
	2.0	0.583835	0.401818	0.31569	0.276811	0.0609546	0.422876	0.434448	3.44383
	3.0	0.684533	0.507068	0.401818	0.337647	0.038482	0.286572	0.0722435	2.92154

4. Estimation and Simulation

In this section, we obtain the mathematical expressions of the maximum likelihood estimators (MLEs) $(\hat{\theta}_{MLE}, \hat{\gamma}_{MLE})$ of the WC-Weibull distribution. Besides deriving of the mathematical expression of $\hat{\theta}_{MLE}$, and $\hat{\gamma}_{MLE}$, we also provide a simulation study to assess their performances (numerically and visually).

4.1. Estimation

Assume a set (size n) of random samples, say $T_1, T_2, \ldots, T_n$, taken from $f(t;\boldsymbol{\eta})$ of the WC-Weibull distribution defined by Equation (5). Corresponding to $f(t;\boldsymbol{\eta})$, the likelihood function (LF), say $\lambda(\theta,\gamma|t_t, t_2, \ldots, t_n)$, is given by

$$\lambda(\theta,\gamma|t_t, t_2, \ldots, t_n) = \prod_{i=1}^{n} f(t_i;\boldsymbol{\eta}). \tag{13}$$

Using Equation (5) in Equation (13), we obtain

$$\lambda(\theta,\gamma|t_t, t_2, \ldots, t_n) = \prod_{i=1}^{n} \frac{\pi\theta\gamma t_i^{\theta-1} e^{-\gamma t_i^{\theta}} \sin\left[\frac{\pi\left(1-e^{-\gamma t_i^{\theta}}\right)}{2-e^{-\gamma t_i^{\theta}}}\right]}{(e-1)\left[2-e^{-\gamma t_i^{\theta}}\right]^2} e^{\left(1-\cos\left[\frac{\pi\left(1-e^{-\gamma t_i^{\theta}}\right)}{2-e^{-\gamma t_i^{\theta}}}\right]\right)}. \tag{14}$$

Corresponding to $\lambda(\theta,\gamma|t_t, t_2, \ldots, t_n)$ in Equation (14), the log LF (LLF), say $\ell(\theta,\gamma)$, is given by

$$\begin{aligned}
\ell(\theta,\gamma) &= n\log\pi + n\log\theta + n\log\gamma + (\theta-1)\sum_{i=1}^{n}\log t_i - \gamma\sum_{i=1}^{n} t_i^{\theta} - n\log(e-1) \\
&\quad - 2\sum_{i=1}^{n}\log\left[2-e^{-\gamma t_i^{\theta}}\right] + \sum_{i=1}^{n}\log\sin\left[\frac{\pi\left(1-e^{-\gamma t_i^{\theta}}\right)}{2-e^{-\gamma t_i^{\theta}}}\right] \\
&\quad + \sum_{i=1}^{n}\left(1-\cos\left[\frac{\pi\left(1-e^{-\gamma t_i^{\theta}}\right)}{2-e^{-\gamma t_i^{\theta}}}\right]\right).
\end{aligned}$$

The partial derivatives of $\ell(\theta,\gamma)$ are given by

$$\begin{aligned}
\frac{\partial}{\partial\theta}\ell(\theta,\gamma) &= \frac{n}{\theta} + \sum_{i=1}^{n}\log t_i - \gamma\sum_{i=1}^{n}(\log t_i)t_i^{\theta} - 2\gamma\sum_{i=1}^{n}\frac{(\log t_i)t_i^{\theta}e^{-\gamma t_i^{\theta}}}{\left[2-e^{-\gamma t_i^{\theta}}\right]} \\
&\quad + \pi\gamma\sum_{i=1}^{n}\cot\left[\frac{\pi\left(1-e^{-\gamma t_i^{\theta}}\right)}{2-e^{-\gamma t_i^{\theta}}}\right]\frac{(\log t_i)t_i^{\theta}e^{-\gamma t_i^{\theta}}}{\left(2-e^{-\gamma t_i^{\theta}}\right)^2} \\
&\quad + \pi\gamma\sum_{i=1}^{n}\sin\left[\frac{\pi\left(1-e^{-\gamma t_i^{\theta}}\right)}{2-e^{-\gamma t_i^{\theta}}}\right]\frac{(\log t_i)t_i^{\theta}e^{-\gamma t_i^{\theta}}}{\left(2-e^{-\gamma t_i^{\theta}}\right)^2},
\end{aligned}$$

and

$$\begin{aligned}
\frac{\partial}{\partial\gamma}\ell(\theta,\gamma) &= \frac{n}{\gamma} - \sum_{i=1}^{n} t_i^{\theta} - \sum_{i=1}^{n}\frac{2t_i^{\theta}e^{-\gamma t_i^{\theta}}}{\left[2-e^{-\gamma t_i^{\theta}}\right]} + \pi\sum_{i=1}^{n}\cot\left[\frac{\pi\left(1-e^{-\gamma t_i^{\theta}}\right)}{2-e^{-\gamma t_i^{\theta}}}\right]\frac{t_i^{\theta}e^{-\gamma t_i^{\theta}}}{\left(2-e^{-\gamma t_i^{\theta}}\right)^2} \\
&\quad + \pi\sum_{i=1}^{n}\sin\left[\frac{\pi\left(1-e^{-\gamma t_i^{\theta}}\right)}{2-e^{-\gamma t_i^{\theta}}}\right]\frac{t_i^{\theta}e^{-\gamma t_i^{\theta}}}{\left(2-e^{-\gamma t_i^{\theta}}\right)^2}.
\end{aligned}$$

Equating $\frac{\partial}{\partial\theta}\ell(\theta,\gamma)$ and $\frac{\partial}{\partial\gamma}\ell(\theta,\gamma)$ to zero, and solving, we obtain, respectively, the MLEs $(\hat{\theta}_{MLE}, \hat{\gamma}_{MLE})$ of the parameters (θ,γ) of the WC-Weibull distribution. As we can see, the expressions $\frac{\partial}{\partial\theta}\ell(\theta,\gamma)$ and $\frac{\partial}{\partial\gamma}\ell(\theta,\gamma)$ of the WC-Weibull distribution are not in explicit forms. So, to ensure the uniqueness of $\hat{\theta}_{MLE}$ and $\hat{\gamma}_{MLE}$, we obtain the profiles of their LLF; see Section 5.

4.2. Simulation

This subsection evaluates the behaviors of $\hat{\theta}_{MLE}$ and $\hat{\gamma}_{MLE}$ of the WC-Weibull distribution. The evaluation of $\hat{\theta}_{MLE}$ and $\hat{\gamma}_{MLE}$ was performed by conducting a simulation study (SS). The SS was conducted with the help of R-script, by means of generating random numbers from the WC-Weibull distribution using the inverse CDF approach.

The SS was carried out for $\theta = 1.4, \gamma = 1.0$, $\theta = 0.9, \gamma = 1.2$, and $\theta = 1.1, \gamma = 0.8$. For a random sample of size, say $n = 50, 100, 150, 200, \ldots, 1000$, the simulation results were simulated 1000 times. Out of these 1000 iterations, the simulation results were reported for $n = 50, 100, 200, 300, 400, 500, 600, 700, 800, 900, 1000$.

We considered two statistical measures as decisive tools to observe the performances of $\hat{\theta}_{MLE}$ and $\hat{\gamma}_{MLE}$. These measures included the bias and mean square error (MSE) with mathematical expressions given, respectively, by

$$Bias(\hat{\boldsymbol{\eta}}_{MLE}) = \frac{1}{1000} \sum_{i=1}^{1000} (\hat{\boldsymbol{\eta}}_i - \boldsymbol{\eta}),$$

and

$$MSE(\hat{\boldsymbol{\eta}}_{MLE}) = \frac{1}{1000} \sum_{i=1}^{1000} (\hat{\boldsymbol{\eta}}_i - \boldsymbol{\eta})^2.$$

Corresponding to (i) $\theta = 0.5, \gamma = 1$, (ii) $\theta = 1.5, \gamma = 1$, and (iii) $\theta = 1.5, \gamma = 1$, the simulation results are reported in Tables 2–4 (numerical illustration) and in Figures 2–4 (visual illustration). Based on the given facts in Tables 2–4 and Figures 2–4, we can see that as n increased (i.e., as $n \longrightarrow \infty$), the

- values of $\hat{\theta}_{MLE}$ and $\hat{\gamma}_{MLE}$ became closer to the true values.
- the MSE of $\hat{\theta}_{MLE}$ and $\hat{\gamma}_{MLE}$ decreased to zero.
- the bias of $\hat{\theta}_{MLE}$ and $\hat{\gamma}_{MLE}$ decayed to zero.

Table 2. The simulation results (numerical illustration) of the WC-Weibull distribution for $\theta = 1.4$ and $\gamma = 1$.

w	Parameters	MLEs	MSEs	Biases
50	θ	1.4296460	0.02405948	0.02964635
	γ	1.0431000	0.03529194	0.04309999
100	θ	1.4212070	0.01200113	0.02120715
	γ	1.0130417	0.01491238	0.01304166
200	θ	1.4111950	0.00610701	0.01119543
	γ	1.0108342	0.00682204	0.01083417
300	θ	1.4081410	0.00375586	0.00814085
	γ	1.0101036	0.00518498	0.01010361
400	θ	1.4051080	0.00297678	0.00510784
	γ	1.0051150	0.00348963	0.00511498
500	θ	1.4036400	0.00241264	0.00364035
	γ	1.0023226	0.00277201	0.00232259
600	θ	1.4024130	0.00192576	0.00241314
	γ	1.0052975	0.00220275	0.00529752
700	θ	1.4023780	0.00169136	0.00237846
	γ	0.9983985	0.00209227	−0.00160147
800	θ	1.4015180	0.00132295	0.00151838
	γ	1.0030077	0.00186708	0.00300772
900	θ	1.4025340	0.00123326	0.00253402
	γ	1.0011655	0.00173252	0.00116550
1000	θ	1.4027230	0.00113616	0.00272319
	γ	0.9995966	0.00133558	−0.00040337

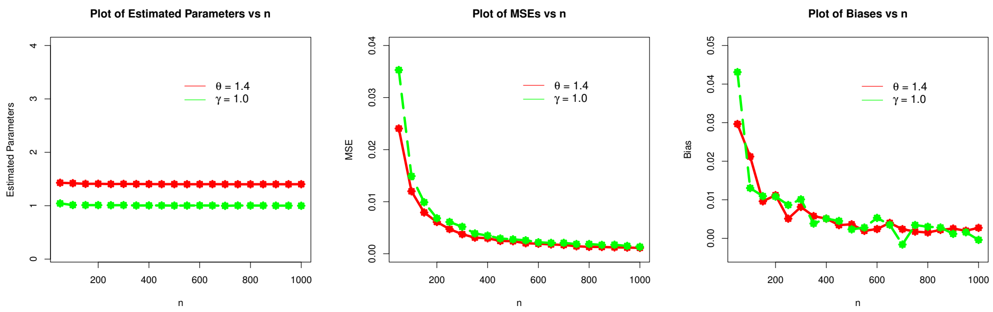

Figure 2. The simulation results (visual illustration) of the WC-Weibull distribution for $\theta = 1.4$ and $\gamma = 1$.

Table 3. The simulation results (numerical illustration) of the WC-Weibull distribution for $\theta = 0.9$ and $\gamma = 1.2$.

w	Parameters	MLEs	MSEs	Biases
50	θ	0.9301292	0.010420608	0.030129186
	γ	1.2587990	0.054114017	0.058799380
100	θ	0.9190032	0.004904806	0.019003196
	γ	1.2302100	0.023946464	0.030209555
200	θ	0.9083318	0.002087803	0.008331841
	γ	1.2147470	0.009057488	0.014747452
300	θ	0.9067783	0.001287310	0.006778291
	γ	1.2107980	0.006254901	0.010797619
400	θ	0.9048156	0.000789564	0.004815557
	γ	1.2079350	0.003876875	0.007935161
500	θ	0.9015265	0.000492410	0.001526458
	γ	1.2020270	0.002638221	0.002026584
600	θ	0.9035450	0.000448842	0.003544961
	γ	1.2037500	0.001965831	0.003750256
700	θ	0.9027654	0.000369818	0.002765412
	γ	1.2025920	0.001510795	0.002592192
800	θ	0.9020800	0.000248739	0.002080045
	γ	1.2008570	0.001217765	0.000856731
900	θ	0.9017151	0.000199939	0.001715065
	γ	1.2028740	0.001146012	0.002873864
1000	θ	0.9026201	0.000202154	0.002620059
	γ	1.2004670	0.000825658	0.000466553

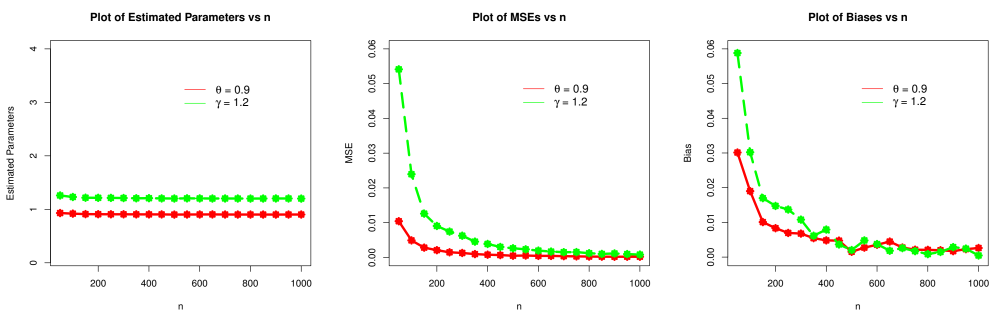

Figure 3. The simulation results (visual illustration) of the WC-Weibull distribution for $\theta = 0.9$ and $\gamma = 1.2$.

Table 4. The simulation results (numerical illustration) of the WC-Weibull distribution for $\theta = 1.1$ and $\gamma = 0.8$.

w	Parameters	MLEs	MSEs	Biases
50	θ	1.1307770	0.017107187	0.030776790
	γ	0.8234098	0.019228798	0.002340984
100	θ	1.1162240	0.007458450	0.016223649
	γ	0.8115002	0.009817093	0.001150019
200	θ	1.1089390	0.003489588	0.008939034
	γ	0.8071731	0.004698275	0.000717306
300	θ	1.1080430	0.002455605	0.008043088
	γ	0.8028852	0.002875517	0.000288516
400	θ	1.1057100	0.001785741	0.005709626
	γ	0.8017098	0.002251494	0.000170975
500	θ	1.1046660	0.001251863	0.004666320
	γ	0.8029802	0.001741128	0.000298020
600	θ	1.1028690	0.001034179	0.002868828
	γ	0.8000814	0.001298472	0.000008142
700	θ	1.1026830	0.000934220	0.002683266
	γ	0.8024500	0.001270398	0.000245001
800	θ	1.1021630	0.000702283	0.002163235
	γ	0.8003387	0.001051193	0.000033872
900	θ	1.1028780	0.000730588	0.002878359
	γ	0.8012919	0.000900604	0.000129185
1000	θ	1.1021200	0.000572035	0.002120053
	γ	0.8009227	0.000773674	0.000009226

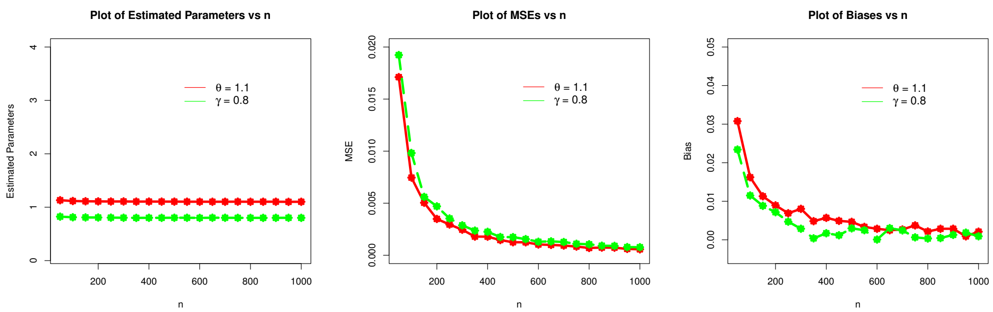

Figure 4. The simulation results (visual illustration) of the WC-Weibull distribution for $\theta = 1.1$ and $\gamma = 0.8$.

5. Applications to Medical Data Sets

In this section, we analyze three practical applications (i.e., three data sets) using the WC-Weibull distribution to illustrate its applicability in the medical sector. These data sets are taken from the medical sector and represent the times until the events occur. In the next subsection, we provide a complete description of these data sets.

5.1. Description of the Data Sets

The first data set (onward, it is expressed as Data 1) represents the remission times of 128 patients. These patients were suffering from bladder cancer. This data set was originally reported by [19].

The second data set (onward, it is expressed as Data 2) represents the survival times of 72 guinea pigs. These pigs were infected with a disease called the virulent tubercle bacilli. In recent times, Data 2 has been considered by numerous researchers, for example, see [20,21].

The third data set (onward, it is expressed as Data 3) represents the survival times of 46 patents. These patients were given chemotherapy treatment. For a more detailed description of Data 3, we refer to [22,23].

Corresponding to Data 1, Data 2, and Data 3, some basic descriptive plots are presented in Figure 5, Figure 6 and Figure 7, respectively. These descriptive plots are:

- Kernel density, which provides a smooth curve that represents the distribution of the data, allowing for insights into its shape, central tendency, and variability.
- Histogram, which is a basic graphical representation of the distribution of a variable. It divides the range of values into intervals, or bins, and displays the frequency or density of data points falling within each bin.
- Box plot, which provides a concise summary of the distribution of a variable. It displays key statistical measures, including the median, quartiles, and potential outliers.
- Violin plot, which combines the features of a box plot and a kernel density plot. It presents a mirrored density plot on each side of a central box plot, providing insights into both the summary statistics and the distributional shape of the data.

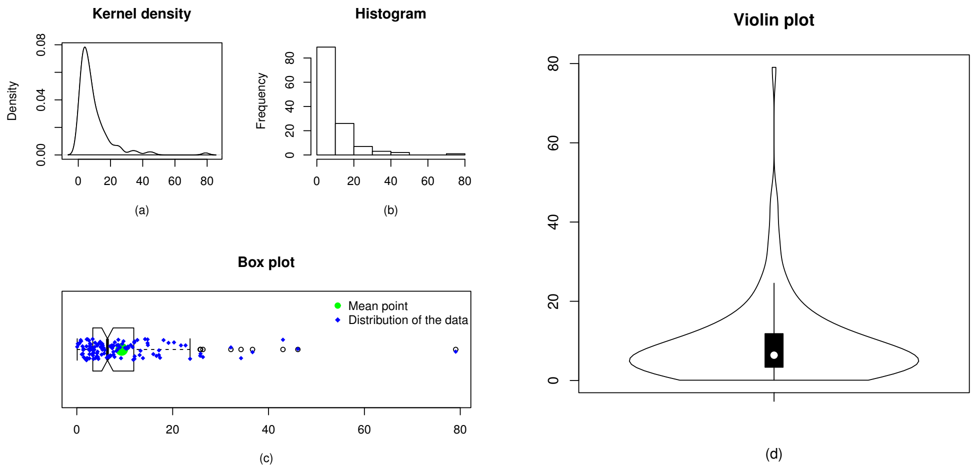

Figure 5. The kernel density (**a**), histogram (**b**), box plot (**c**), and violin plot (**d**) of Data 1.

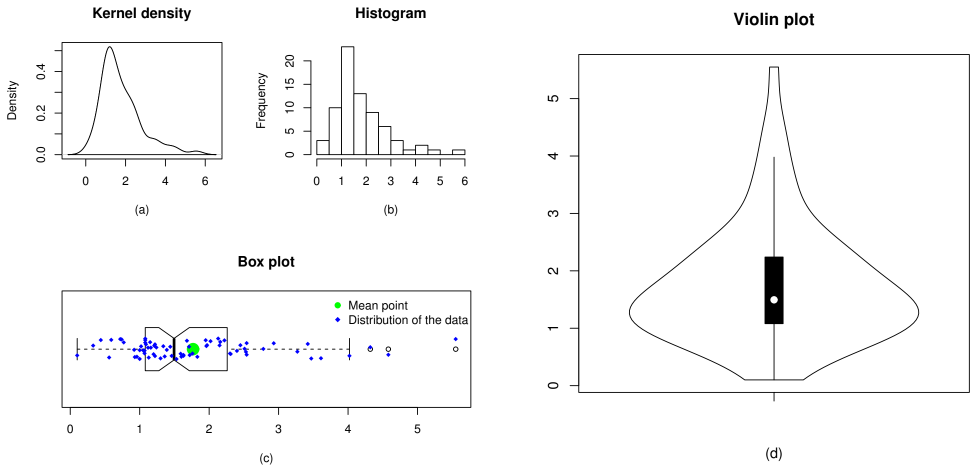

Figure 6. The kernel density (**a**), histogram (**b**), box plot (**c**), and violin plot (**d**) of Data 2.

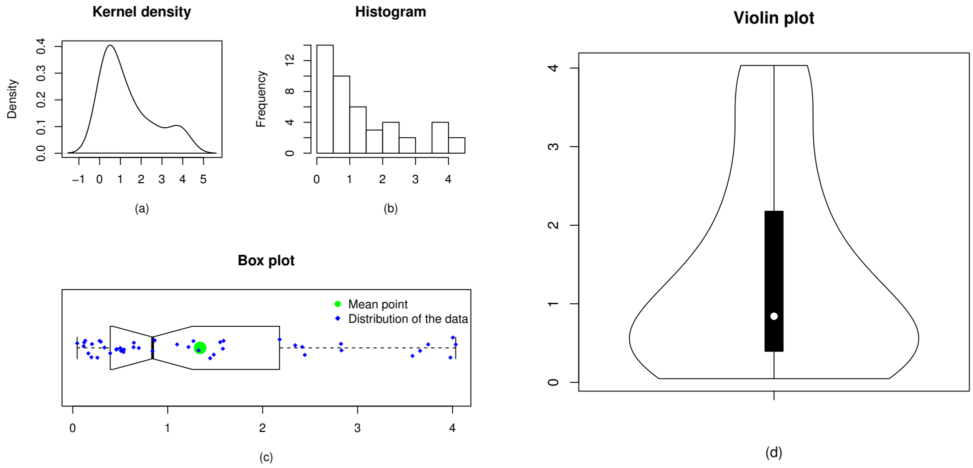

Figure 7. The kernel density (**a**), histogram (**b**), box plot (**c**), and violin plot (**d**) of Data 3.

5.2. The Rival Distributions

In this subsection, we discuss some rival distributions that were selected to compare with the WC-Weibull distribution using the medical data sets (i.e., Data 1, Data 2, and Data 3). These distributions were selected with the aim of showing the superior fitting power of the WC-Weibull distribution over some existing distributions in the literature. The rival distributions included the following: (i) Weibull distribution, (ii) new extended exponential Weibull (NEE-Weibull) distribution, and (iii) new alpha cosine Weibull (NAC-Weibull) distribution. The Weibull distribution was considered as a rival distribution of the proposed model because the proposed model is an extension of the Weibull distribution. The reasoning behind this was to show whether the proposed model performed better than the Weibull distribution or not. The other two competitive distributions were selected as they also have the Weibull distribution as a baseline model.

The CDFs of these rival distributions are given, respectively, by

$$G(t;\boldsymbol{\eta}) = 1 - e^{-\gamma t^{\theta}}, \qquad t \geq 0, \theta, \gamma > 0,$$

$$G(t;\beta,\boldsymbol{\eta}) = 1 - \frac{\beta e^{-\gamma t^{\theta}}}{\beta + 1 - e^{-\gamma t^{\theta}}}, \qquad t \geq 0, \theta, \gamma, \beta > 0,$$

and

$$G(t;\alpha,\boldsymbol{\eta}) = \frac{\alpha^{\cos\left(\frac{\pi}{2} e^{-\gamma t^{\theta}}\right)} - 1}{\alpha - 1}, \qquad t \geq 0, \theta, \gamma, \alpha > 0, \alpha \neq 1.$$

5.3. The Decisive Tools

This subsection offers a description of the decisive tools that were implemented to check the performances of the WC-Weibull and other rival distributions. The decisive tools that were considered in this paper consisted of information criteria (IC) and goodness-of-fit tests. The IC included the following: Akaike IC (AIC) with mathematical expression $2k - 2\ell(.)$, Consistent AIC (CAIC) calculated by $\frac{2nk}{n-k-1} - 2\ell(.)$, Bayesian IC (BIC) obtained by $k\log(n) - \ell(.)$ and Hannan–Quinn IC (HQIC) with mathematical formula $2k\log[\log(n)] - 2\ell(.)$.

In the formulae of IC, the term k represents the model parameter(s), n indicates the sample size, and $\ell(.)$ represents the LLF. The goodness-of-fit tests included the following:

- Anderson Darling (AD) test, having the mathematical formula

$$-n - \frac{1}{n}\sum_{i=1}^{n}(2i-1)[\log G(t_i) + \log(1 - G(t_{n-i+1}))],$$

- Cramer-Von-Messes (CM) test, computed as

$$\frac{1}{12n} + \sum_{i=1}^{n} \left[\frac{2i-1}{2n} - G(t_i) \right]^2,$$

- Kolmogorov-Smirnov (KS) test, obtained as

$$sup_t[G_n(t) - G(t)].$$

In the formulae of the goodness-of-fit tests, the terms i represent the ith sample in the data, when the data is ordered in an increasing way, $G_n(t)$ represents the empirical CDF, $G(t)$ is the CDF of a probability distribution and sup_t represents the supremum of the set of distances between $G_n(t)$ and $G(t)$. In addition to the above decisive tools, the p-value was also computed for all the fitted distributions.

Among the possible set of probability distributions, the best-suited distribution was the one in which the numerical values of the decisive tools was lower and in which the p-value was higher than in its rival distributions.

5.4. Analysis of First Real Data Set

In this subsection, we provide the numerical results of the MLEs, decisive tools, and some visual description of the fitting power of the WC-Weibull and the rival distributions using Data 1.

Corresponding to Data 1, the values of $\hat{\theta}_{MLE}$, $\hat{\gamma}_{MLE}$, $\hat{\beta}_{MLE}$, and $\hat{\alpha}_{MLE}$ of the fitted models are reported in Table 5. The visual illustration of the profiles of the LLF of $\hat{\theta}_{MLE}$ and $\hat{\gamma}_{MLE}$ of the WC-Weibull distribution are provided in Figure 8. These plots show the uniqueness of the $\hat{\theta}_{MLE}$ and $\hat{\gamma}_{MLE}$ of the WC-Weibull distribution. Figure 8 reveals that the estimated parameters were the maximization of the LLF of the WC-Weibull distribution.

Using Data 1, the values of the decisive measures of the fitted distributions are provided in Table 6. For the WC-Weibull distribution, the values of the decisive measures were CM = 0.0568, AD = 0.3645, KS = 0.0497, p-value = 0.9089, AIC = 826.3411, CAIC = 826.4371, BIC = 832.0452, and HQIC = 828.6587. Looking at Table 6, we can see that the WC-Weibull distribution had the lowest values of the decisive measures and a high p-value, as compared to the rival distributions. Thus, from Table 6, we can easily conclude that the WC-Weibull distribution was the best model for Data 1.

Furthermore, we also considered different graphical approaches to confirm the close-fitting capability of the WC-Weibull distribution. For the graphical comparison, we obtained the plots of the estimated PDF, Kaplan–Meier survival plot, and empirical CDF; see Figures 9 and 10. The visual illustrations in Figures 9 and 10, show that the WC-Weibull distribution closely fit Data 1.

Table 5. The numerical values of $\hat{\theta}_{MLE}$, $\hat{\gamma}_{MLE}$, $\hat{\beta}_{MLE}$, and $\hat{\alpha}_{MLE}$ along with standard errors (presented in the parenthesis) of the fitted models for Data 1.

Dist.	$\hat{\theta}$	$\hat{\gamma}$	$\hat{\beta}$	$\hat{\alpha}$
WC-Weibull	0.85133 (0.05379)	0.18984 (0.02808)	-	-
Weibull	1.05357 (0.06668)	0.09165 (0.01832)	-	-
NEE-Weibull	1.20118 (0.20839)	0.04084 (0.02911)	0.92755 (0.52344)	-
NAC-Weibull	0.75268 (0.10561)	0.17150 (0.07296)	-	8.00968 (8.67012)

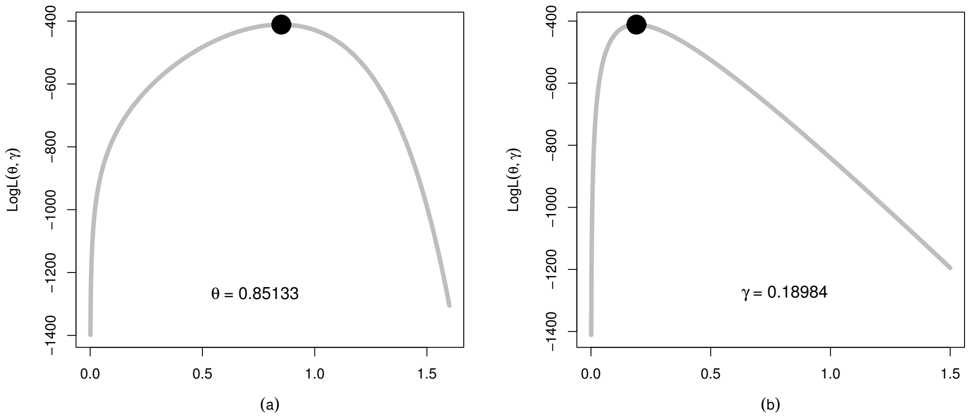

Figure 8. The plots for the (**a**) log-likelihood profile of $\hat{\theta}_{MLE}$ and (**b**) log-likelihood profile of $\hat{\gamma}_{MLE}$ of the WC-Weibull distribution for Data 1.

Table 6. The values of the decisive tools of the WC-Weibull and its rival probability distributions for Data 1.

Dist.	CM	AD	KS	p-Value	AIC	CAIC	BIC	HQIC
WC-Weibull	0.0568	0.3645	0.0497	0.9089	826.3411	826.4371	832.0452	828.6587
Weibull	0.1324	0.7925	0.0742	0.4798	832.1903	832.2863	837.8943	834.5078
NEE-Weibull	0.0816	0.5073	0.0625	0.6993	831.1741	831.3676	837.7302	834.3505
NAC-Weibull	0.1248	0.7378	0.0667	0.6185	833.1293	833.3229	841.6854	836.6057

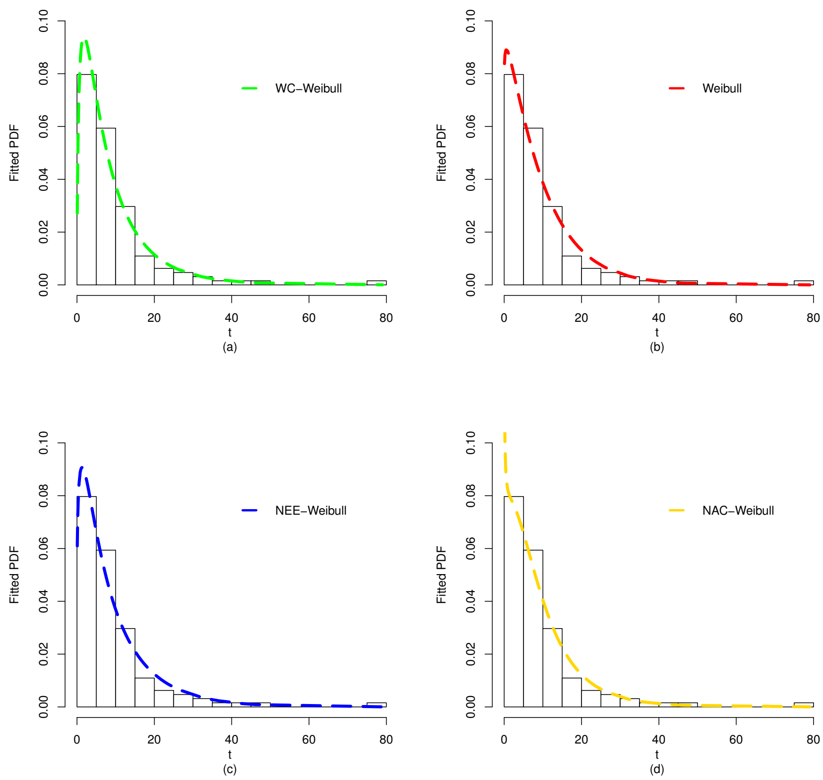

Figure 9. The plots for the fitted PDF of (**a**) WC-Weibull distribution, (**b**) Weibull distribution, (**c**) NEE-Weibull distribution, and (**d**) NAC-Weibull distribution for Data 1.

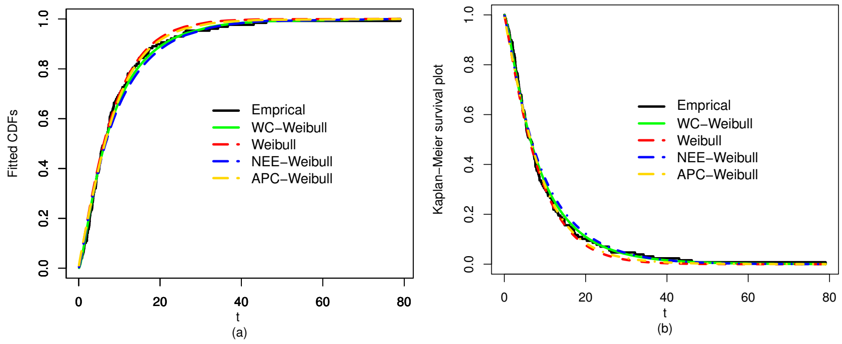

Figure 10. The plots for the (**a**) fitted CDF and (**b**) fitted SF of the WC-Weibull and rival models for Data 1.

5.5. Analysis of Second Real Data Set

In this subsection, we analyze Data 2 to show the superior performance of the WC-Weibull distribution using the decisive measures and graphical illustration.

Using Data 2, the values of $\hat{\theta}_{MLE}, \hat{\gamma}_{MLE}, \hat{\beta}_{MLE}$, and $\hat{\alpha}_{MLE}$ of the WC-Weibull distribution and rival models are provided in Table 7. Corresponding to Data 2, the uniqueness of $\hat{\theta}_{MLE}$ and $\hat{\gamma}_{MLE}$ of the WC-Weibull distribution is shown visually in Figure 11. The plots in Figure 11 show that the estimated parameters were the maximization of the LLF of the WC-Weibull distribution.

Based on Data 2, the comparative results of the WC-Weibull distribution and competing distributions are presented in Table 8. For Data 2, the decisive measures of the WC-Weibull distribution were the following: CM = 0.1008, AD = 0.1008, KS = 0.0931, p-value = 0.5602, AIC = 192.5671, CAIC = 192.7410, BIC = 197.1205, and HQIC = 194.3798. Based on Table 8, it is obvious that the WC-Weibull distribution again outperformed the Weibull, NEE-Weibull, and NAC-Weibull distributions.

For Data 2, the plots of the estimated PDF, Kaplan–Meier survival plot, and empirical CDF of the WC-Weibull, Weibull, NEE-Weibull, and NAC-Weibull distributions are provided in Figures 12 and 13. These plots again confirmed the close-fitting capability of the WC-Weibull distribution for Data 2.

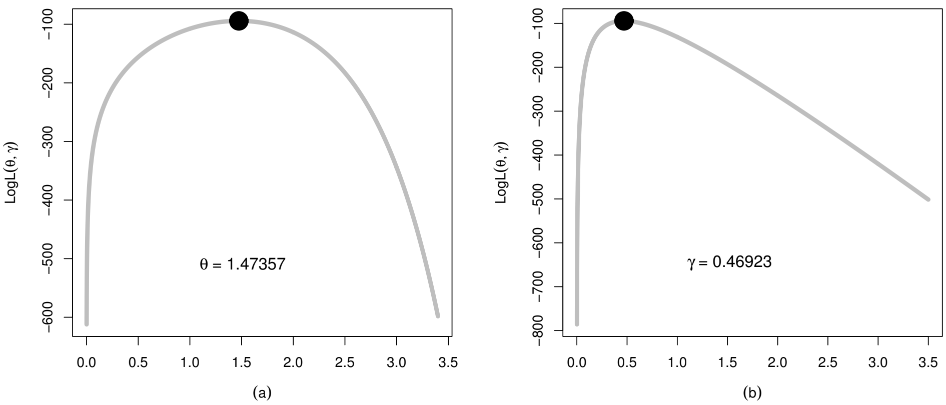

Figure 11. The plots for the (**a**) log-likelihood profile of $\hat{\theta}_{MLE}$ and (**b**) log-likelihood profile of $\hat{\gamma}_{MLE}$ of the WC-Weibull distribution for Data 2.

Table 7. The numerical values of $\hat{\theta}_{MLE}, \hat{\gamma}_{MLE}, \hat{\beta}_{MLE}$, and $\hat{\alpha}_{MLE}$ along with standard errors (presented in the parenthesis) of the fitted models for Data 2.

Dist.	$\hat{\theta}$	$\hat{\gamma}$	$\hat{\beta}$	$\hat{\alpha}$
WC-Weibull	1.47357 (0.12474)	0.46923 (0.06400)	-	-
Weibull	1.82376 (0.15865)	0.28374 (0.054179)	-	-
NEE-Weibull	2.34318 (0.61212)	0.07853 (0.11671)	0.31447 (0.55515)	-
NAC-Weibull	1.22748 (0.20337)	0.45063 (0.14358)	-	13.81467 (15.71335)

Table 8. The values of the decisive tools of the WC-Weibull and its rival probability distributions for Data 2.

Dist.	CM	AD	KS	*p*-Value	AIC	CAIC	BIC	HQIC
WC-Weibull	0.1008	0.6203	0.0931	0.5602	192.5671	192.7410	197.1205	194.3798
Weibull	0.1647	0.9702	0.1051	0.4032	195.5797	195.7536	200.1331	197.3924
NEE-Weibull	0.1191	0.6590	0.1069	0.3821	194.5930	194.9460	200.4230	196.3121
NAC-Weibull	0.1565	0.9033	0.1018	0.4444	196.4686	196.8215	203.2986	199.1876

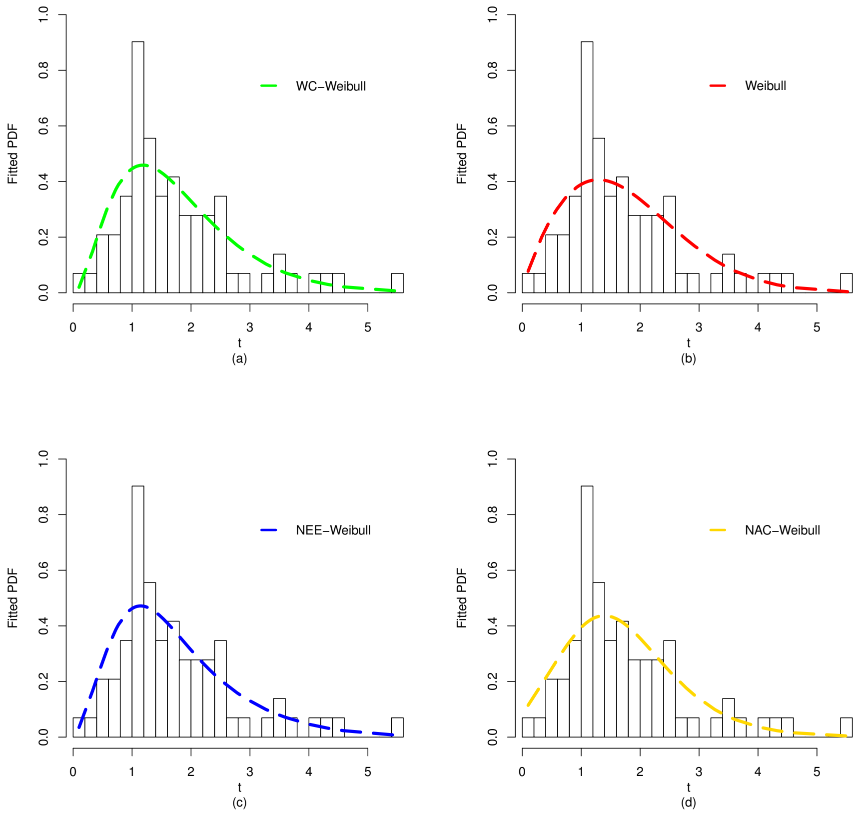

Figure 12. The plots for the fitted PDF of (**a**) WC-Weibull distribution, (**b**) Weibull distribution, (**c**) NEE-Weibull distribution, and (**d**) NAC-Weibull distribution for Data 2.

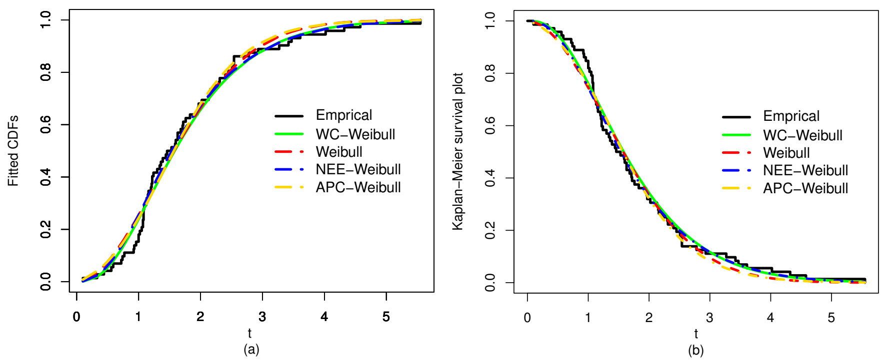

Figure 13. The plots for the (**a**) fitted CDF and (**b**) fitted SF of the WC-Weibull and rival models for Data 2.

5.6. Analysis of Third Real Data Set

This subsection offers the third illustration of the WC-Weibull distribution using Data 3. We again compare the fitting results of the WC-Weibull distribution with rival distributions.

For Data 3, the values of $\hat{\theta}_{MLE}$, $\hat{\gamma}_{MLE}$, $\hat{\beta}_{MLE}$, and $\hat{\alpha}_{MLE}$ of the WC-Weibull distribution with rival distributions are displayed in Table 9. To confirm the uniqueness of $\hat{\theta}_{MLE}$ and $\hat{\gamma}_{MLE}$ of the WC-Weibull distribution, the plots of the profiles of their LLF are provided in Figure 14. Figure 14 shows that the estimated parameters maximized the LLF of the WC-Weibull distribution.

After analyzing Data 3, the fitting results of the WC-Weibull, Weibull, NEE-Weibull, and NAC-Weibull distributions are provided in Table 10. From Table 10, the values of the decisive measures of the WC-Weibull distribution were given by CM = 0.0618, AD = 0.4282, KS = 0.0936, p-value = 0.7909, AIC = 119.7899, CAIC = 120.0756, BIC = 123.4032, and HQIC = 121.1369. The numerical results in Table 10, again confirmed the superior fitting of the WC-Weibull distribution.

In addition to the third illustration of the WC-Weibull distribution in Table 10, we again provide a visual comparison to assess its performance. Corresponding to Data 3, the fitted plots are provided in Figures 15 and 16. The fitted plots show that the WC-Weibull distribution also fit Data 3 very closely.

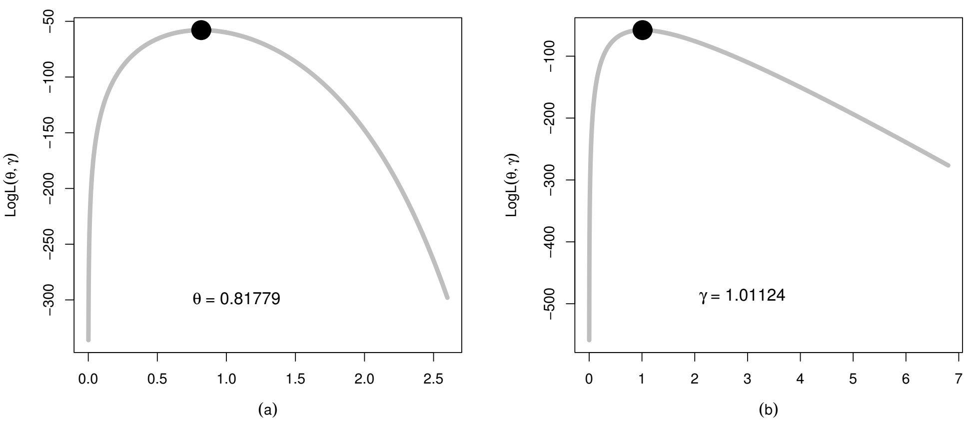

Figure 14. The plots for the (**a**) log-likelihood profile of $\hat{\theta}_{MLE}$ and (**b**) log-likelihood profile of $\hat{\gamma}_{MLE}$ of the WC-Weibull distribution for Data 3.

Table 9. The numerical values of $\hat{\theta}_{MLE}$, $\hat{\gamma}_{MLE}$, $\hat{\beta}_{MLE}$, and $\hat{\alpha}_{MLE}$ along with standard errors (presented in the parenthesis) of the fitted models for Data 3.

Dist.	$\hat{\theta}$	$\hat{\gamma}$	$\hat{\beta}$	$\hat{\alpha}$
WC-Weibull	0.81779 (0.08997)	1.01124 (0.13157)	-	-
Weibull	1.05460 (0.15865)	0.71613 (0.05417)	-	-
NEE-Weibull	1.26571 (0.20517)	0.38501 (0.21702)	0.62759 (0.73089)	-
NAC-Weibull	1.08096 (0.20755)	0.33115 (0.19496)	-	0.49814 (0.89409)

Table 10. The values of the decisive tools of the WC-Weibull and its rival probability distributions for Data 3.

Dist.	**CM**	**AD**	**KS**	***p*-Value**	**AIC**	**CAIC**	**BIC**	**HQIC**
WC-Weibull	0.0618	0.4282	0.0936	0.7909	119.7899	120.0756	123.4032	121.1369
Weibull	0.0813	0.5439	0.1102	0.6055	122.2476	122.5334	125.8610	123.5947
NEE-Weibull	0.0661	0.4523	0.0986	0.7215	121.6609	122.2462	127.0808	123.6814
NAC-Weibull	0.0803	0.5377	0.1115	0.5913	122.2846	122.8700	127.7046	124.3052

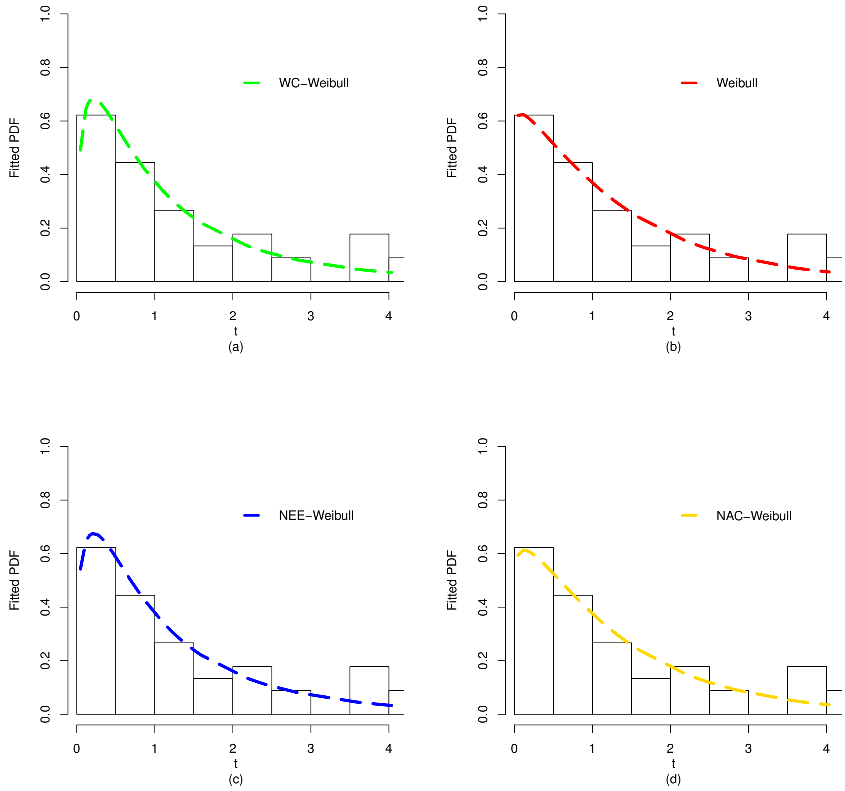

Figure 15. The plots for the fitted PDF of (**a**) WC-Weibull distribution, (**b**) Weibull distribution, (**c**) NEE-Weibull distribution, and (**d**) NAC-Weibull distribution for Data 3.

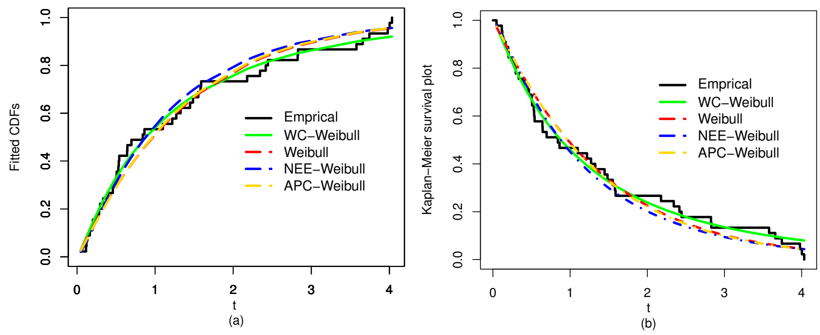

Figure 16. The plots for the (**a**) fitted CDF and (**b**) fitted SF of the WC-Weibull and rival models for Data 3.

6. Conclusions

In this paper, a new methodology was adopted and implemented to introduce a new probabilistic approach without any additional parameters. The proposed distributional method is called the weighted cosine-*G* family of distribution. The weighted cosine-*G* method was introduced by using the cosine function with the aim of avoiding re-parametrization problems. Some distributional properties of the WC-*G* models were derived. The MLEs of the WC-*G* distributions were obtained and their performances assessed through different simulation studies. To illustrate the WC-*G* family, a special model, called the weighted cosine-Weibull distribution, was developed. The practical importance of the WC-Weibull distribution was shown by analyzing three time-to-event data set. These data sets were taken from the medical sector. The first data set represented the remission times of bladder cancer patients. The second data set represented the survival times of guinea pigs infected with virulent tubercle bacilli. The third data set represented the survival times of chemotherapy patents. Based on eight different statistical procedures, it was established that the WC-Weibull distribution is a reasonable distribution to apply in modeling the medical data sets involved.

Author Contributions: Conceptualization, O.H.O., H.M.A. and Z.A.; methodology, O.H.O., H.M.A. and Z.A.; software, H.M.A., Z.A. and G.S.R.; validation, O.H.O. and Z.A.; formal analysis, O.H.O., H.M.A., Z.A. and G.S.R.; investigation, O.H.O.; data curation, Z.A. and G.S.R.; writing—original draft preparation, O.H.O., H.M.A., Z.A. and G.S.R.; writing—review and editing, O.H.O., H.M.A. and Z.A.; visualization, O.H.O., Z.A. and G.S.R. All authors have read and agreed to the published version of the manuscript.

Funding: This research was funded by the Deanship of Scientific Research at Princess Nourah bint Abdulrahman University, through the Research Funding Program, Grant No. (FRP-1444-10).

Data Availability Statement: The data is available from the corresponding author upon reasonable request.

Conflicts of Interest: The authors declare no conflict of interest.

References

1. Almarashi, A.M.; Algarni, A.; Nassar, M. On estimation procedures of stress-strength reliability for Weibull distribution with application. *PLoS ONE* **2020**, *15*, e0237997. [CrossRef] [PubMed]
2. Zhao, W.; Khosa, S.K.; Ahmad, Z.; Aslam, M.; Afify, A.Z. Type-I heavy tailed family with applications in medicine, engineering and insurance. *PLoS ONE* **2020**, *15*, e0237462. [CrossRef] [PubMed]
3. Al-Babtain, A.A.; Kumar, D.; Gemeay, A.M.; Dey, S.; Afify, A.Z. Modeling engineering data using extended power-Lindley distribution: Properties and estimation methods. *J. King Saud Univ.-Sci.* **2021**, *33*, 101582. [CrossRef]
4. Gómez, Y.M.; Gallardo, D.I.; Bourguignon, M.; Bertolli, E.; Calsavara, V.F. A general class of promotion time cure rate models with a new biological interpretation. *Lifetime Data Anal.* **2023** , *29*, 66–86. [CrossRef] [PubMed]
5. Gamage, P.W.W.; McMahan, C.S.; Wang, L. A flexible parametric approach for analyzing arbitrarily censored data that are potentially subject to left truncation under the proportional hazards model. *Lifetime Data Anal.* **2023** , *29*, 188–212. [CrossRef]
6. Alghamdi, S.M.; Shrahili, M.; Hassan, A.S.; Gemeay, A.M.; Elbatal, I.; Elgarhy, M. Statistical Inference of the Half Logistic Modified Kies Exponential Model with Modeling to Engineering Data. *Symmetry* **2023**, *15*, 586. [CrossRef]
7. Alsadat, N.; Ahmad, A.; Jallal, M.; Gemeay, A.M.; Meraou, M.A.; Hussam, E.; Elmetwally, E.M.; Hossain, M.M. The novel Kumaraswamy power Frechet distribution with data analysis related to diverse scientific areas. *Alex. Eng. J.* **2023**, *70*, 651–664. [CrossRef]
8. Tashkandy, Y.A.; Nagy, M.; Akbar, M.; Mahmood, Z.; Gemeay, A.M.; Hossain, M.M.; Muse, A.H. The Exponentiated Cotangent Generalized Distributions: Characteristics and Applications Patients of Chemotherapy Treatments Data. *IEEE Access* **2023**, *11*, 35697–35709. [CrossRef]
9. Chesneau, C.; Bakouch, H.S.; Hussain, T. A new class of probability distributions via cosine and sine functions with applications. *Commun. Stat.-Simul. Comput.* **2019**, *48*, 2287–2300. [CrossRef]
10. Almalki, S.J.; Yuan, J. A new modified Weibull distribution. *Reliab. Eng. Syst. Saf.* **2013**, *111*, 164–170. [CrossRef]
11. Kumar, D.; Singh, U.; Singh, S.K. A new distribution using sine function-its application to bladder cancer patients data. *J. Stat. Appl. Probab.* **2015**, *4*, 417.
12. Mahmood, Z.; Chesneau, C.; Tahir, M.H. A new sine-G family of distributions: Properties and applications. *Bull. Comput. Appl. Math.* **2019**, *7*, 53–81.
13. Ampadu, C.B. The hyperbolic Tan-X family of distributions: Properties, application and characterization. *J. Stat. Model. Theory Appl.* **2021**, *2*, 1–13.
14. Norton, E.C. The inverse hyperbolic sine transformation and retransformed marginal effects. *Stata J.* **2022**, *22*, 702–712. [CrossRef]
15. Kormos, M.; Vörös, D.; Zaránd, G. Finite-temperature dynamics in gapped one-dimensional models in the sine-Gordon family. *Phys. Rev. B* **2022**, *106*, 205151. [CrossRef]
16. Tomy, L.; Chesneau, C. Applications of the Sine Modified Lindley Distribution to Biomedical Data. *Math. Comput. Appl.* **2022**, *27*, 43. [CrossRef]
17. Rajkumar, J.; Sakthivel, K.M. A New Method of Generating Marshall–Olkin Sine–G Family and Its Applications in Survival Analysis. *Lobachevskii J. Math.* **2022**, *43*, 463–472. [CrossRef]
18. Nanga, S.; Nasiru, S.; Dioggban, J. Cosine Topp–Leone family of distributions: Properties and Regression. *Res. Math.* **2023**, *10*, 2208935. [CrossRef]
19. Lee, E.T.; Wang, J. *Statistical Methods for Survival Data Analysis*; John Wiley & Sons: Hoboken, NJ, USA, 2003; Volume 476.
20. Kemaloglu, S.A.; Yilmaz, M. Transmuted two-parameter Lindley distribution. *Commun. Stat.-Theory Methods* **2017**, *46*, 11866–11879. [CrossRef]
21. Khosa, S.K.; Afify, A.Z.; Ahmad, Z.; Zichuan, M.; Hussain, S.; Iftikhar, A. A new extended-f family: Properties and applications to lifetime data. *J. Math.* **2020**, *2020*, 5498638. [CrossRef]

22. Bekker, A.; Roux, J.J.J.; Mosteit, P.J. A generalization of the compound Rayleigh distribution: Using a Bayesian method on cancer survival times. *Commun. Stat.-Theory Methods* **2000**, *29*, 1419–1433. [CrossRef]
23. Nwezza, E.E.; Ugwuowo, F.I. An extended normal distribution for reliability data analysis. *J. Stat. Manag. Syst.* **2022**, *25*, 369–392. [CrossRef]